Voltammetric Studies of Through-Space and Through-Bond Electrostatic Interactions in Alkyl Linked Ferrocene and Benzoaza-15-crown-5 Receptor Molecules in Acetonitrile

Shan Jin,[†] Xianbo Jin,[†] Dihua Wang,[†] Gongzhen Cheng,[†] Ling Peng,[†,‡] and George Z. Chen*[,†,§]

College of Chemistry and Molecular Science, Wuhan University, Wuhan 430072 People's Republic of China, Departement de chimie, AFMB CNRS UMR 6098, 163, avenue de Luminy, 13288 Marseille, France, and School of Chemical, Environmental and Mining Engineering, University of Nottingham, University Park, Nottingham NG7 2RD, U.K.

Received: December 23, 2004; In Final Form: March 15, 2005

Six new ferrocene alkyl-benzoaza-15-crown-5 molecules with different alkyl spacer lengths were synthesized and investigated by voltammetry in acetonitrile. Their mean potentials ($E^{\circ\prime}$) were more negative than that of ferrocene. The changes were greater for the bis-substituted ligands than for the monosubstituted ones. Increasing the alkyl spacer length shifted $E^{\circ\prime}$ negatively from $-CH_2-$ to $-(CH_2)_2-$ but positively from $-(CH_2)_2-$ to $-(CH_2)_4-$. This unusual variation is attributed to the combined electron donating and withdrawing influences and also the steric effect from the substituents on the ferrocene moiety. Analyses of the potentials of the molecules and their fully protonated forms suggested intramolecular electrostatic signaling through not only the space but also the alkyl chain which is usually considered to be an insulator for through-bond communication. Diffusion coefficients with insignificant differences between the receptors and their fully protonated forms were derived from cyclic voltammograms, suggesting insignificant further conformational variation upon protonation.

Introduction

Redox responsive receptors[1] can be bifunctional molecular devices that are driven by electrochemical means and capable of, for example, transporting ionic species between immiscible liquid phases[2] and sensing/recognizing guest species with high selectivity.[3] They can also be used as practical models to study intramolecular interactions for a better and more quantitative understanding of the properties of the framework and environment of complex macromolecules in condensed phases.[4] In the simplest case, a redox responsive receptor consists of a redox active group, a guest affinitive group, and a linker group. In Figure 1, the three groups correspond respectively to the ferrocene, the benzoaza-15-crown-5 macrocycle, and the alkyl chain with the amide or the tertiary amine end group in the intermediate and final products of the synthesis reactions. The linker, together with the local environment around the molecule, enables electron and guest transfer to and from the molecule in a coupled and mutual influencing manner via a mechanism such as through-space and/or through-bond electrostatic interactions and/or conformational changes.[1,5]

As reviewed in a number of recent articles,[1,5] past research on redox responsive receptors aimed mainly to synthesize molecules possessing a desired binding strength, selectivity, and sensitivity and to use them for applications such as sensors, phase transfer catalysts, and switches. The coupling mechanism has been extensively studied in terms of thermodynamics and electrostatics, but mechanistic and kinetic issues, which can affect practical uses, have to be dealt with, in many cases, individually. For example, the redox group is usually selected from those capable of simple and reversible electron transfer reactions, for example, ferrocene and quinone. However, electron transfer can be perturbed differently by connecting guest binding substituents to the redox group, depending on, to a great extent, the linking bond being saturated or conjugated, electron-rich or -deficient, bulky or flexible, and oxidizable or reducible. Knowledge of such complications is crucial for understanding guest binding induced physicochemical changes in and future technological uses of these redox responsive receptors. On this front, some early examples indicated qualitatively or semiquantitatively Coulombic interactions within the complex molecules, but recent work has attempted to reach a more quantitative understanding.[4,6−8]

Ferrocene based redox responsive receptors are possibly the earliest and most widely studied, mainly due to ferrocene offering satisfactory electrochemical reversibility and synthetic stability.[1c,3a] Recently, we have shown quantitatively that the coordination chemistry and electrochemistry of receptors **3**a−**3**c and **6**a−**6**c in Figure 1 are coupled by *intramolecular electrostatic interactions* and the mean potential ($E^{\circ\prime}$) of the molecule varies upon cation binding in well accordance with Coulomb's law.[6c] Of particular interest is the observation of such interactions becoming ineffective beyond about a 1 nm spacer length, implying at least a threefold importance. First, it may help to create a better understanding of some biological processes involving intramolecular electrostatic interactions, for example, protein folding[9] and antigen−antibody recognition.[10] Second, the knowledge of a limited interaction distance is crucial in developing molecular or *nanometer* devices to be operated by intramolecular electrostatic forces.[11] Third, the nanometer effect, which is well recognized when material dimensions decrease, may also be true when molecule sizes increase.

This paper presents a detailed account of the synthesis and electrochemical properties of **3**a−**3**c and **6**a−**6**c, which are

* Corresponding author. E-mail: george.chen@nottingham.ac.uk.
[†] Wuhan University.
[‡] AFMB CNRS UMR 6098.
[§] University of Nottingham.

10.1021/jp044149z CCC: $30.25
Published on Web 05/06/2005

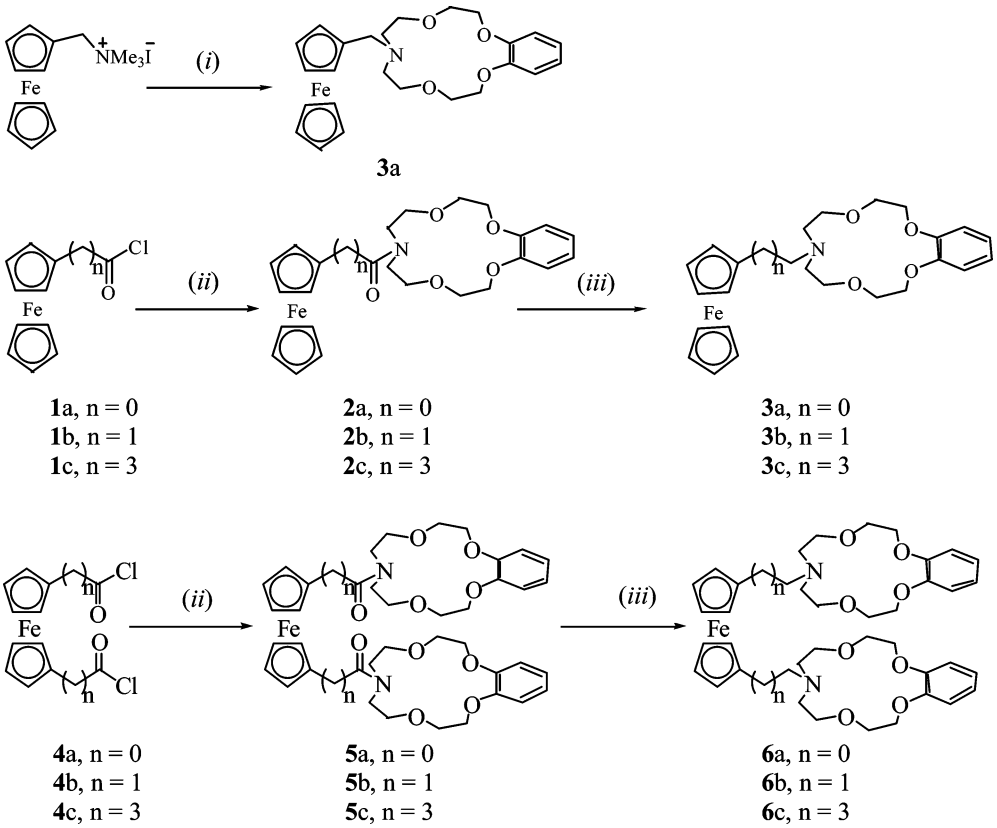

Figure 1. Schematic representations of synthesis reactions and molecular structures of the alkyl linked ferrocene benzoaza-15-crown-5 receptor molecules **3**a−**3**b and **6**a−**6**b: (*i*) benzoaza-15-crown-5, K_2CO_3, and CH_3CN; (*ii*) benzoaza-15-crown-5, NEt_3, and toluene; (*iii*) CH_2Cl_2/THF (1:2) and $LiAlH_4$.

conceptually familiar but experimentally new.[4,7,8] Attention is paid to the effect of varying the substituents on the electrochemistry of the ferrocene center. In addition, details of the influence of acid addition on the voltammetry of the molecules are reported. (Research has been done or is ongoing with **2**a−**2**c and **5**a−**5**c in Figure 1 and also with the metal cation binding behavior of these receptors, but the results will be addressed separately.) An interesting and unprecedented finding from comparing values of $E^{\circ\prime}$ is that not only through-space but also through-bond intramolecular electrostatic interactions may be present in these molecules, even though the alkyl chain is commonly perceived as an insulator for electrostatic communication. The through-bond interaction can be incorporated into a variable relative permittivity in Coulomb's law. Further, diffusion coefficients are estimated from the voltammetric data and indicate, at least on the voltammetric time scale, insignificant conformational changes in these molecules upon protonation (and hence electric repulsion). This finding again differs from our initial thought based on literature information[7a,b] that these molecules are conformationally unstable in solution because they consist of flexible substituents that may rotate around the ferrocene moiety under influence (also see later discussion in this paper).

Experimental Section

Instrumentation and Chemicals. NMR spectra were measured using a Varian Mercury-300 spectrometer at 300 MHz for ^{1}H NMR and 75.45 MHz for ^{13}C NMR. MALDI-TOF-MS were obtained using 2,5-dihydroxybenzoic acid as the matrix and were measured on a Biflex III spectrometer. Column chromatography was performed on neutral alumina (neutral, 100−200 mesh) or silica. Electrochemical measurements were performed on a CHI660A potentiostat (CH Instruments Company, U.S.A.). A three-electrode cell was used to contain the solution of the compound and supporting electrolyte in dry acetonitrile. Deaeration of the solution was achieved by argon bubbling through the solution for about 10 min before measurement. During experiments, the cell was sealed from air and the argon flow escaped from the cell via a liquid (silicon oil) seal. The ligand and electrolyte (^{n}Bu$_4$NPF$_6$) concentrations were typically 0.001 and 0.1 mol dm^{-3}, respectively. A 500 μm diameter platinum disk working electrode, a platinum wire counter electrode, and a Ag/Ag$^+$ reference electrode were used. The Ag/Ag$^+$ electrode contained an internal solution of 0.01 mol dm^{-3} $AgNO_3$ in acetonitrile and was incorporated with a salt bridge containing 0.1 mol dm^{-3} Bu_4NPF_6 in acetonitrile. The electrochemical experiments were carried out at room temperature and pressure. All chemicals were of the AnalaR grades unless otherwise specified. Where necessary, solvents were purified prior to use and stored under nitrogen. Acetonitrile was predried over class 4 Å molecular sieves (4−8 mesh) and then distilled under nitrogen from CaH_2 or P_2O_5. Toluene, ether, and tetrahydrofuran (THF) were distilled from Na/benzophenone; CH_2Cl_2 was distilled from P_2O_5; and *N*,*N*,*N*′,*N*′-tetramethylethylenediamine, pyridine, and Et_3N were distilled from and stored over KOH. 1-Chlorocarbonylalkyl ferrocene (**1**a−**1**c), 1,1′-bis(chlorocarbonylalkyl) ferrocene (**4**a−**4**c),[12−14] and benzoaza-15-crown-5 were prepared according to the literature procedures.[15]

Synthesis. The synthesis reactions of **3**a−**3**c and **6**a−**6**c are presented in Figure 1 and described below.

Ferrocene Carbonyl-Benzoaza-15-crown-5 (2a). A solution of **1**a (130 mg, 0.52 mmol) in toluene was added dropwise over 20 min to a stirred solution of benzoaza-15-crown-5 (155 mg,

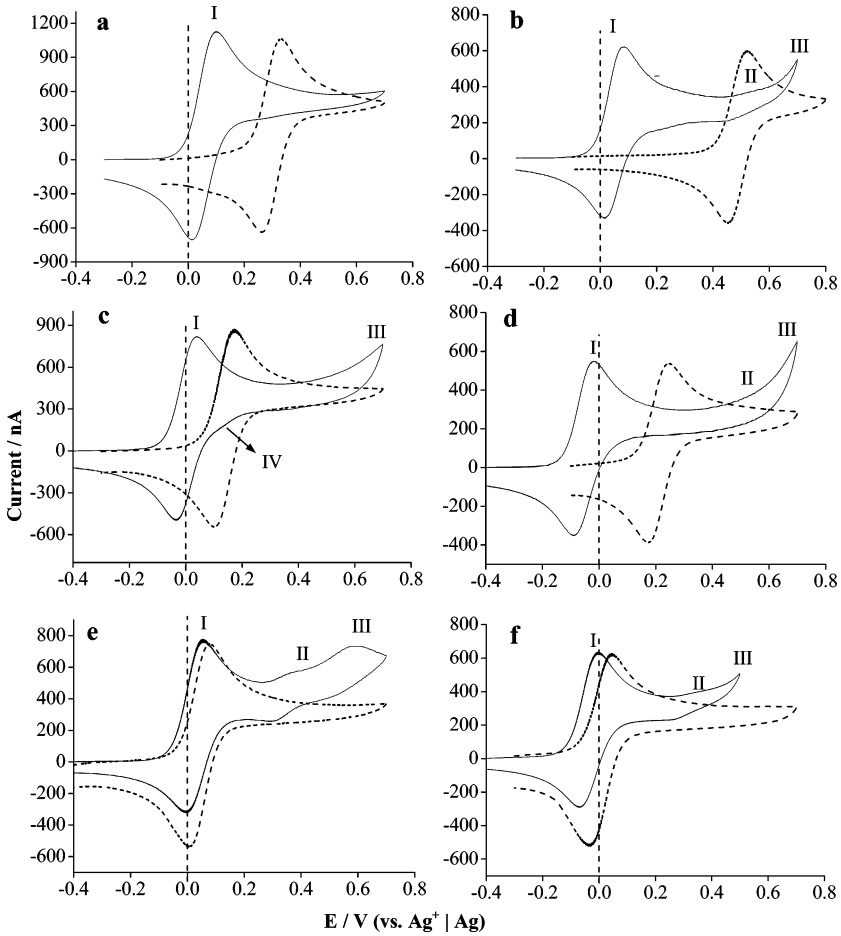

Figure 2. CVs of (a) **3**a, (b) **6**a, (c) **3**b, (d) **6b**, (e) **3**c, and (f) **6**c in acetonitrile in the absence (solid line) and presence (dashed line) of an excess amount (>4 equiv) of HPF_6 (60% in water). Scan rate, 100 mV s^{-1}; ligand concentration, varying but close to 1.5 ± 0.3 mmol dm^{-3}.

0.58 mmol) and triethylamine (0.2 mL) in toluene under nitrogen. The mixture was further stirred for 4 h before filtration and evaporation under reduced pressure. The residue was dissolved in CH_2Cl_2 and washed with water, and the solvent was removed before being chromatographed on an alumina column using CH_2Cl_2 and CH_2Cl_2/methanol (98:2) as the eluant. An orange semisolid (**2**a) was isolated in 80% yield.

Ferrocene Bis(carbonylbenzoaza-15-crown-5) (5a). An analogous synthetic procedure to the preparation of **2**a was employed using **4**a (214 mg, 0.7 mmol), benzoaza-15-crown-5 (374 mg, 1.4 mmol), and triethylamine (0.2 mL). **5**a was obtained as an orange semisolid in 85% yield.

2b, 2c, 5b, and 5c. Preparation was analogous to that of **2**a and **5**a.

Ferrocene Mono(methylene benzoaza-15-crown-5) (3a). A solution of trimethylammo-niometryferrocene iodide[16] (210 mg, 0.64 mmol) in dry acetonitrile (20 mL) was added dropwise over 15 min to a refluxing solution of benzoaza-15-crown-5 (152 mg, 0.57 mmol) in acetonitrile (20 mL) containing anhydrous potassium carbonate (790 mg, 5.7 mmol). The mixture was further refluxed for 36 h. After cooling, the mixture was filtered and the solids washed with CH_2Cl_2. The solvent was removed from the organic extracts under reduced pressure, the residue dissolved in CH_2Cl_2 and washed with water, and the solvent removed before being chromatographed on an alumina column using CH_2Cl_2 and CH_2Cl_2/methanol (98:2) as eluant. An orange semisolid (**3**a) was isolated in 60% yield.

Ferrocene Bis(methylene benzoaza-15-crown-5) (6a). **5**a (120 mg, 0.15 mmol) was dissolved in dry CH_2Cl_2 (5 mL) containing dry THF (10 mL) under N_2 with $LiAlH_4$ (65 mg, 1.71 mmol). The reaction mixture was refluxed for 3 h, then diluted with CH_2Cl_2, and quenched with deionized water. The solvent was evaporated in a vacuum. The residue was chromatographed over an alumina column using CH_2Cl_2 and CH_2Cl_2/methanol (99:1) as eluant. The isolated product (**6**a) was a yellow oil in 90% yield.

3a−3c, 6b, and 6c. Preparation was analogous to that of **6**a starting with **2**a−**2**c, **5**b, and **5**c, respectively.

It should be mentioned that two methods were used to prepare **3**a in this work. NMR and voltammetry confirmed no difference for **3**a from the two routes. All the isolated final products have good solubility in common organic solvents, such as dichloromethane, chloroform, and acetonitrile. They were characterized by ^1H NMR, ^{13}C NMR, and MALDI-TOF-MS spectroscopic (see the Supporting Information) and electrochemical analyses. All the analytical and spectra data are consistent with the predicted structures.

Results and Discussion

Basic Voltammetric Properties. *Ferrocene Center.* All cyclic voltammograms (CVs) of **3**a−**3**c and **6**a−**6**c (~1×10^{-3} mol dm^{-3}) in dry acetonitrile exhibited a quasi-reversible peak couple **I** in the potential range from −0.4 to 0.3 V (vs Ag/Ag^+), which can be ascribed to the ferrocene center. Figure 2 compares the CVs recorded under similar conditions. The oxidation and reduction peak potentials (E_{pa} and E_{pc}) were typically separated by about 70 mV, which is close to that of simple ferrocene measured in acetonitrile. The oxidation peak current (i_{pa}) was found to vary linearly with ligand concentration

and also with the square root of the scan rate between 10 and 300 mV s^{-1}, while E_{pa} and E_{pc} remained almost unchanged; see Figure 3a and b. These CV features were repeated on the square-wave voltammograms (SWVs).

Tertiary Amine(s). However, the CVs also exhibit minor features of complications. The ratio of the reduction and oxidation peak currents, i_{pc}/i_{pa}, of couple **I** was approximately 1 at high potential scan rates, but becomes smaller with decreasing scan rate. For example, the ratios for **3**a were 1.0, 0.9 and 0.8 at scan rates of 400, 100 and 10 mVs^{-1}, respectively. This is evidence of a slow chemical change following the electron transfer (oxidation).

At potentials more positive than 0.3 V, a small wave couple **II** was observed on some CVs (Figure 2b, e, and f). For all receptor molecules, an irreversible oxidation current **III** appeared beyond 0.55 V (Figure 2b and d−f). Upon protonation or metal cation complexation, both couple **II** and current **III** disappeared, accompanied by improved CV reversibility (see Figure 2 which also compares CVs of the free ligands with those of their fully protonated forms).

These minor complications were previously reported for analogous molecules and attributed to the combined effects of (1) the lone electron pair on the nitrogen atom of the tertiary amine(s), which is more influential to ferrocenium than ferrocene, and (2) the slow oxidation of amines with weak product adsorption to the electrode.[8c,17] It is interesting to mention that these minor features were similar between ligand molecules of different alkyl spacer lengths, indicating that amine oxidation bears perhaps more responsibility than the lone electron pair. This is because the influence of the latter is expected to decline with increasing distance from the ferrocene center. Also, the potentials of both **II** and **III** become less positive with increasing alkyl spacer length, which is evidence of these minor voltammetric features being indeed from the same molecule as the ferrocene center, instead of impurities. The ferrocene oxidation at lower potentials introduces a positive charge into the molecule, making the amine oxidation more difficult. Obviously, the shorter the alkyl spacer, the more positive potential needed to oxidize the amine.

Influence of Residual Water. On some of the CVs, another small but noticeable wave couple **IV** is seen after couple **I**; see Figure 2c. Couple **IV** was not always clearly observed, even for the same ligand. When it did appear, usually more prominent at low potential scan rates, its potential remained approximately the same for the same ligand but varied from ligand to ligand. For example, although couple **IV** on the CV of **3**a in Figure 2 is not clearly visible, it was observed in some other experiments at about 230 mV more positive than couple **I** (see Figure 5a). On a few CVs of **3**b, couple **IV** was seen as shoulders about 120 mV more positive than couple **I**.

On the basis of the random appearance of couple **IV**, its more positive potential than that of the ferrocene center, and that all the solutions were prepared in air, moisture, that might have entered the acetonitrile solution before the experiment, is considered to be the likely cause. In the presence of water, the tertiary amine in the ligand can undergo hydrolysis as described below.

$$R_3N + H_2O \rightarrow R_3NH^+ + OH^- \qquad (I)$$

The proton on nitrogen can then shift the ferrocene oxidation positively. Nevertheless, the limited amount of water in the solution means a small fraction of the ligand molecules undergoing hydrolysis and hence the small size of couple **IV**. Particularly, for the bis-substituted ligands, only one of the two tertiary amines may be protonated via reaction I. The hydrolysis hypothesis is supported by experiments in which the CVs were recorded, respectively, when the ligand solution was freshly prepared and after the solution was left overnight in air. The CV from the overnight solution was dominated by couple **IV**. Further evidence came from purposely protonated ligands whose potentials agreed with those of couple **IV** (see later discussion on protonation in this paper).

Mean Potential and Substitution. Of particular relevance to this work is the variation of the mean potential, $E^{\circ\prime} = (E_{pa} + E_{pc})/2$, of couple **I** with changing the number and length of the alkyl spacers linking the macrocycle(s) to the ferrocene center. Table 1 lists the potential data of all six ligands, measured against the Ag/Ag^+ reference electrode. For the convenience of discussion, the measured potentials are also converted against the ferrocene/ferrocenium (Fc/Fc^+) couple in Table 1. It should be mentioned that, in current literature,[1,3−5] the symbol $E_{1/2}$ is often used for the mean potential but, in strict electrochemical terms, represents the half-wave potential on a steady-state voltammogram, for example, the polarogram. Nevertheless, it is true that the two are the same or very close in value for reversible and quasi-reversible systems.

The $E^{\circ\prime}$ values of the substituted ferrocenes are all more negative than that of simple ferrocene, which is expected from the electron donating effect of the alkyl substituents.[18] Additional effects may come from the benzoaza-crown-ether ring because of the lone electron pair on the nitrogen atom of the tertiary amine(s)[5a,17c,19a] and the electron-rich oxygen atoms and benzene ring. These attributions agree with the fact that the bis-substituted ligands exhibit larger negative potential shifts, approximately doubled, than their monosubstituted counterparts. However, further comparison between the data in Table 1 reveals an interesting trend: $E^{\circ\prime}$ shifts negatively from $-CH_2-$ (**3**a and **6**a) to $-(CH_2)_2-$ (**3**b and **6**b) and then positively from $-(CH_2)_2-$ (**3**b and **6**b) to $-(CH_2)_4-$ (**3**c and **6**c).

In acetonitrile, it is known that each methyl substituent can negatively shift the $E^{\circ\prime}$ value of ferrocene by about 50 mV.[18a,20] A reasonable approximation is that each further addition of the $-CH_2-$ subunit to the alkyl chain may shift the potential by a value of −5 to −10 mV. For example, the reported potential difference is 40 mV between $Fc-(CH_2)_7-CH_3$ and the longer $Fc-(CH_2)_{11}-CH_3$ in an aqueous electrolyte.[18b]

Combining the effects from the alkyl spacer and the lone electron pair of the nitrogen atom, one can estimate, with a linear approximation, that the $E^{\circ\prime}$ values of $Fc-(CH_2)_n-NR_2$ should not be very different from −60, −70, and −85 mV (vs Fc/Fc^+) for $n = 1$, 2, and 4, respectively. However, the measured $E^{\circ\prime}$ values of **3**a−**3**c differ from these estimations by about ±25 mV. This difference is much larger for the bis-substituted ligands and unlikely due to the possible maximum experimental errors (±5 mV). It therefore suggests the presence of other effects. The consideration then goes naturally to the effect from the macrocycle ring, including the nitrogen atom.

The nitrogen atom not only has the lone electron pair but is also more electronegative than carbon. Therefore, the $-CH_2-NR_2$ substituent should have a weaker electron donating effect than the $-CH_2-CH_3$ substituent. The electronegative influence of the nitrogen is obviously through-bond and, because of the saturated nature of the alkyl chain, becomes less effective quickly for $n \geq 2$. On the other hand, the greater electronegativity of nitrogen means that its lone electron pair becomes "more negative" in charge density when it is bound to carbon. Apparently, in $Fc-(CH_2)_n-NR_2$, the lone electron pair influence is through-space and declines gradually with increasing n value.

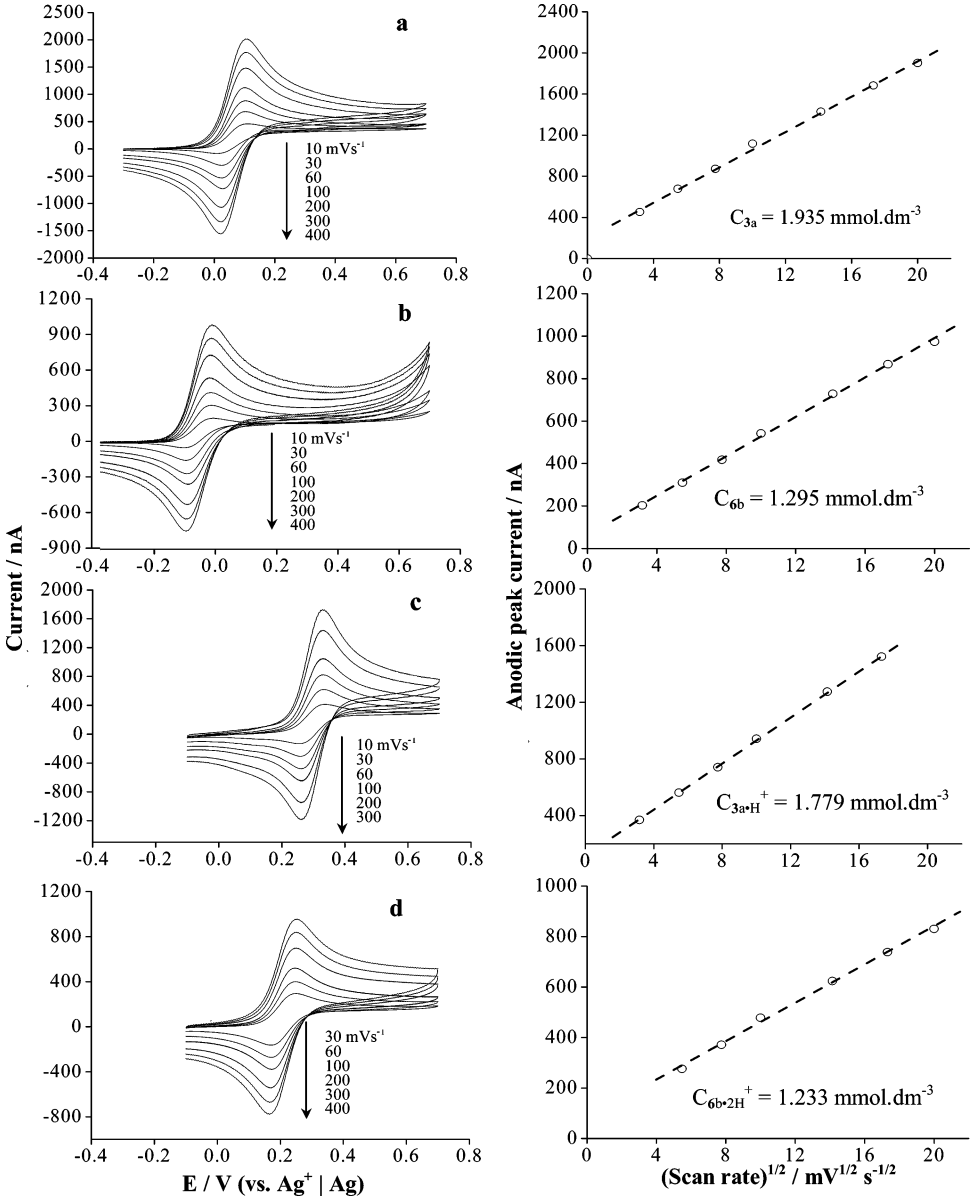

Figure 3. CVs of (a) **3**a and (b) **6**b and their fully protonated forms (c) **3**a.H^+ and (d) **6**b.$2H^+$ at different scan rates as indicated. The linear relationship between the oxidation peak current and the square root of the scan rate is shown on the right-hand side of each of the CVs with indication of the ligand concentration.

Substituents, particularly large ones, can exert steric effects on the property of ferrocene. They can make the oxidized ferrocene (or ferrocenium) center more difficult to access by, for example, anionic species that are required to counterbalance the positive charge.[21] This means a positive shift of the mean potential. In agreement with this analysis, positive potential shifts are commonly observed for neutral ferrocene derivatives when complexed with or included in neutral macrocyclic ligands such as cyclodextrins.[22] For the ligands studied here, the steric effect is largely from the macrocycle moiety, although that from the alkyl spacer may also be present. Therefore, when the alkyl spacer length increases, the access to the ferrocene center by anionic species (PF_6^- in this work) may become slightly more hindered, but the difference is not expected to be significant. In summary, Table 2 lists the four different factors and their possible influences on the potential shift of the ferrocene center.

On the basis of the above analysis, the $E^{\circ\prime}$ variation trend of the ligand molecules can be qualitatively accounted for as follows, in comparison with the Fc$-(CH_2)_n-CH_3$ analogues. In **3**a, all four factors mentioned in Table 2 are present, but the through-bond nitrogen electronegative effect is dominant and hence the less negative $E^{\circ\prime}$ value in comparison with that of Fc-CH_2-CH_3. With an additional $-CH_2-$ subunit in **3**b, the nitrogen electronegative influence is significantly reduced, but the electron donating effect of the alkyl spacer is recovered in addition to that from the lone electron pair of nitrogen, leading to a more negative mean potential than that of Fc$-(CH_2)_2-CH_3$. The presence of four $-CH_2-$ subunits eliminates effectively the nitrogen electronegative influence in **3**c and also greatly reduces the lone electron pair influence. Consequently, because of the substituent's steric effect, the $E^{\circ\prime}$ value of **3**c is slightly more positive than that of Fc$-(CH_2)_4-CH_3$. The same analysis applies to **6**a$-$**6**c.

From the above discussion, it can be concluded that the major reason for **3**b and **6**b to have more negative $E^{\circ\prime}$ values than their neighbors is the electronegativity of the nitrogen atom which functions most significantly at its neighboring $-CH_2-$

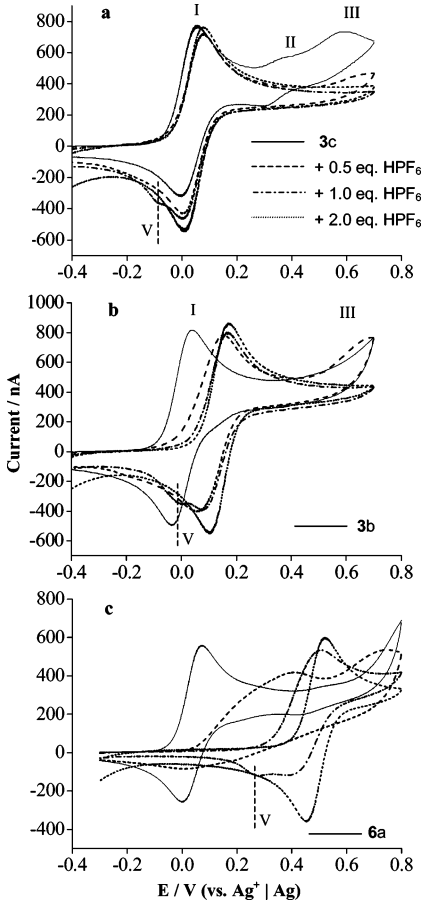

Figure 4. CVs of (a) **3**c, (b) **3**b, (c) and **6**a in the presence of the indicated amounts of HPF_6. Scan rate, 100 mV s^{-1}.

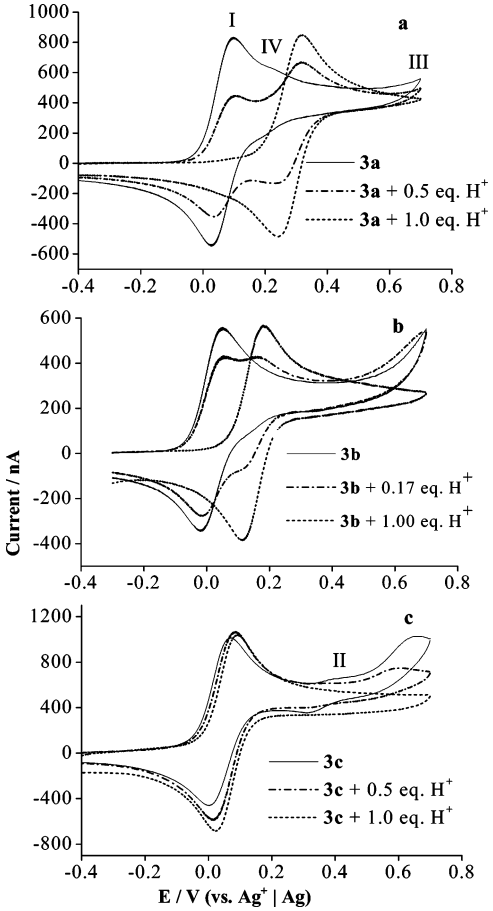

Figure 5. CVs of (a) **3**a, (b) **3**b, and (c) **3**c in acetonitrile recorded upon progressive addition of the monohydrate solid *p*-toluenesulfonic acid. Scan rate, 100 mV s^{-1}.

subunit and is the strongest in **3**a and **6**a. It will be shown later that the electronegative effect also explains well the trend of the positive potential shifts of the ligands in response to the protonation of the tertiary amine groups.

Protonation Induced Voltammetric Changes. In most cases of this work, the aqueous solution of 60% HPF_6 was used to protonate the tertiary amines in the ligands. For comparison, the solid monohydrate *p*-toluenesulfonic acid was also used to study the monosubstituted ligands.

Monosubstituted Ligands + HPF_6. Upon addition of the aqueous HPF_6, the CVs of **3**c and **3**b showed a continuous positive shift of the anodic peak of couple **I** with the addition of up to about 0.5 equiv (molar ratio); see Figure 4a and b. For **3**b, the potential shift was larger and couple **I** became noticeably broader initially and narrower later. With further acid addition, the CV became more reversible in shape and the i_{pc}/i_{pa} ratio increased toward 1 with the peak current increasing linearly with the square root of the scan rate; see Figure 3c and d. Also, the minor couple **II** and current **III** disappeared. These changes are in good agreement with the tertiary amine being protonated and not oxidizable in the same potential window. It should be mentioned that, for both **3**c and **3**b, the positive shift of the anodic peak **I** stopped after 1 equiv of acid addition, accompanied by the disappearance of couple **II** and current **III**. However, the cathodic branch of the CV behaved in a slightly more complex manner, for example, the occurrence of peak **V**, and the changes ceased at an acid addition noticeably higher than 1 equiv. Interestingly, after more than 1 equiv of acid addition, couple **I** of **3**b shifted to about the same position as couple **IV** seen on the CV of the free ligand, see Figure 2c, which agrees with the suggested origin from protonation via reaction I.

For **3**a, the addition of around 0.5 equiv of HPF_6 led to a broad wave that resembled two poorly resolved redox processes. With further HPF_6 addition, the broad wave became more resolved into two peaks: the smaller one centered at the same potential as the free ligand wave and the larger one at more positive potentials. The CV eventually stopped changing and exhibited a very reversible shape after more than 1 equiv of HPF_6 was added.

Bis-Substituted Ligands + HPF_6. The acid induced change on the CV of **6**c followed a similar pattern to that of **3**c. The difference is that the potential shift for **6**c was more prominent. For **6**b, the acid addition led to changes very similar to that of **3**a. For both **6**c and **6**b, the changes in the anodic CV branches ceased after the addition of 2 equiv of acid.

More complicated voltammetric variations were observed for **6**a, as shown in Figure 4c. With addition of up to 1 equiv, the CV shape was seriously distorted with the anodic branch being broadened and the cathodic branch becoming very much similar to that of an irreversible process. With further acid additions, the CVs recovered gradually to the reversible shape at more positive potentials.

Monosubstituted Ligands + Monohydrate p-Toluenesulfonic Acid. Since the aqueous HPF_6 solution contained about 40% water, it would lead to partial protonation of the ligand via reaction I at substoichiometric additions. To gain better insight, CVs were recorded upon progressive additions of the solid monohydrate *p*-toluenesulfonic acid to the solutions of the monosubstituted ligands. The results for **3**c were similar to those

TABLE 1: Electrochemical Data of the Ligands and Their Fully Protonated Forms

	3a	**3**b	**3**c	**6**a	**6**b	**6**c
Fe···N distance[a]/nm	0.456	0.55	0.753	0.456	0.55	0.753
molecule length[b]/nm	0.96	1.05	1.25	1.91	2.10	2.51
$E^{\circ\prime}$ (vs Ag/Ag^+), ligand/mV	67	14	32	48	−47	−29
$E^{\circ\prime}$ (vs Fc/Fc^+), ligand/mV	−22	−76	−56	−41	−136	−118
$E^{\circ\prime}$ (vs Fc/Fc^+), ligand + H^+/mV	208	42	−33	169		
$E^{\circ\prime}$ (vs Fc/Fc^+), ligand + $2H^+$/mV				413	105	−70
$\Delta E^{\circ\prime}$, ligand + H^+/mV	230 (228)[c]	118 (120)[c]	23 (25)[c]	210		
$\Delta E^{\circ\prime}$, ligand + $2H^+$/mV				454	241	48
D ($\times 10^5$, ligand)/$cm^2\ s^{-1}$ ($\pm 0.2 \times 10^5$)	1.0	0.9	0.9	0.6	0.5	0.6
D ($\times 10^5$, ligand + H^+)/$cm^2\ s^{-1}$ ($\pm 0.2 \times 10^5$)	0.9	1.1	1.1			
D ($\times 10^5$, ligand + $2H^+$)/$cm^2\ s^{-1}$ ($\pm 0.2 \times 10^5$)				0.5	0.4	0.6

[a] The data are cited from ref 7. [b] Sum of the Fe···N distance and the estimated diameter of the benzoaza-15-crown-5 ring.[26] [c] Data measured from adding the solid monohydrate *p*-toluenesulfonic acid.

TABLE 2: Possible Negative and Positive Factors and Their Influences on the Mean Potentials of the Ferrocene Centers in $Fc-(CH_2)_n-NR_2$, Including 3a, 3b, and 6a−6c

influencing factor	nature and variation with increasing spacer length
1. alkyl spacer	"−", becoming slightly stronger
2. lone electron pair	"−", decreasing in proportion with (1/distance)^2
3. electronegativity	"+", more significant on the neighboring $-CH_2-$
4. steric effect	"+", becoming slightly stronger and depending on the size of $-NR_2$

of adding HPF_6, as shown in Figures 4a and 5c. However, Figure 5b (for **3**b) presents CVs with clearly two separate peak couples at substoichiometric additions, which differs from the appearance of a broad peak couple as observed when adding the aqueous HPF_6, as shown in Figure 4b (for **3**b). For **3**a, similar differences were observed.

It can be calculated that each equivalent of the added acid contained slightly over 5 equiv of H_2O in the 60% aqueous HPF_6 but only 1 equiv of H_2O in the solid acid. Therefore, hydrolysis can proceed to a greater degree with the addition of HPF_6. It should be pointed out that because hydrolysis cannot occur when all ligand molecules are protonated, its effect should only be prominent at substoichiometric addition levels when free ligand molecules are still available. We therefore believe that hydrolysis is the major reason responsible for the observed difference between adding the two acids.

Another difference between adding the two acids is the appearance of a small reduction peak **V** when substoichiometric amounts of the aqueous HPF_6 were added; see Figure 4. However, peak **V** is absent on all of the CVs in Figure 5. Purposely adding water to the solution after adding the solid acid did not generate peak **V**. Therefore, the origin of peak **V** may be attributed to an impurity in the aqueous HPF_6 solution. Because peak **V** was seen at a potential more negative than that of the free ligand, the impurity may be anionic in nature. Incidentally, it is described in the literature[23a] that aqueous HPF_6 is produced commercially by the reaction between P_2O_5 and anhydrous HF, and the produced HPF_6 is in equilibrium with some fluorophosphoric acids such as HPO_2F_2 and H_2PO_3F, which can dissociate into and are in equilibrium with HF and H_3PO_4.[23b,c] Although we were not able to test these unusual fluorophosphoric acids, we did add $^nBu_4NH_2PO_4^-$ to the solution of **3**b and observed peak **V**.

We would like to emphasize again that the differences between adding the aqueous and solid acids were only seen at substoichiometric additions. At greater additions, almost identical CVs were recorded, which is strong evidence of the potential shifts caused by acid addition truly resulting from the protonation of the tertiary amines.

Through-Bond Intramolecular Electrostatics. The mean potentials ($E^{\circ\prime}$) of the fully protonated ligands, listed in Table 1, follow a different order from that of the free ligands, that is, **3**c.H^+ < **3**b.H^+ < **3**a.H^+ and **6**c.$2H^+$ < **6**b.$2H^+$ < **6**a.$2H^+$. The same order applies to the mean potential differences, $\Delta E^{\circ\prime} = (E^{\circ\prime}_{,\text{protonated}} - E^{\circ\prime}_{,\text{free}})$, between the fully protonated and the respective free ligands. It is worth mentioning that the ratio of the $\Delta E^{\circ\prime}$ values is close to 2 between each bis-substituted ligand and its monosubstituted counterpart. The actual ratios of the potential shifts were 1.97 for **6**a/**3**a, 2.04 for **6**b/**3**b, and 2.09 for **6**c/**3**c, which can be seen as a reflection of the stoichiometric difference in protonation.

The alkyl spacer is usually considered as an insulator for through-bond electrostatic interactions.[5a] Also, a proton is a very small cation and often assumed to be a point charge.[7a,b] If so, the protonation of the ligands should have produced a potential shift approximately the same as a positive point elementary charge at the position of the nitrogen atom. Correlating reported Fe···N distances (measured from crystal structures of very similar molecules[7]) with the sum of the influences of the point charge and the substituents, indicated in Figure 6a by the square and circle symbols, respectively, gives the expected mean potentials of the ferrocene center, as shown by the diamond symbols in the same figure. However, the measured $E^{\circ\prime}$ values of the protonated ligands, indicated by the triangle symbols in Figure 6a, are quite different from the expectation. This discrepancy may be due to the protonation of the tertiary amine leading to a significantly enhanced electron withdrawing power of the nitrogen atom but a slightly reduced effective charge on the bound proton. The former decreases quickly with increasing alkyl spacer length, effectively vanishes beyond two or three $-(CH_2)-$ subunits, but the latter remains approximately constant. Consequently, **3**a exhibits the largest potential shift upon protonation with a significant contribution from through-bond interaction over a single $-CH_2-$ spacer, followed by **3**b, while **3**c shows a positive shift of $E^{\circ\prime}$ that is smaller than that which results from the point elementary charge.

It has been observed for many ferrocene amine compounds[24] and some ferrocene based macrocycle receptors that the cation or proton binding induced $\Delta E^{\circ\prime}$ varies linearly with $1/d$, the reciprocal of the Fe···cation distance.[4,7,8c,d] As an example, Figure 6b draws the linear correlations for the mono- and bis-substituted ligands upon full protonation.[4] Such linear variations have been considered as evidence of the intramolecular interaction being through-space and Coulombic in nature between the bound cation and the oxidized ferrocene center.

The above discussion on the through-bond electrostatic interaction casts a doubt on the through-space interaction understanding. On the basis of experimental measurements, particularly the nonzero common intercepts of the $\Delta E^{\circ\prime} \sim 1/d$ straight

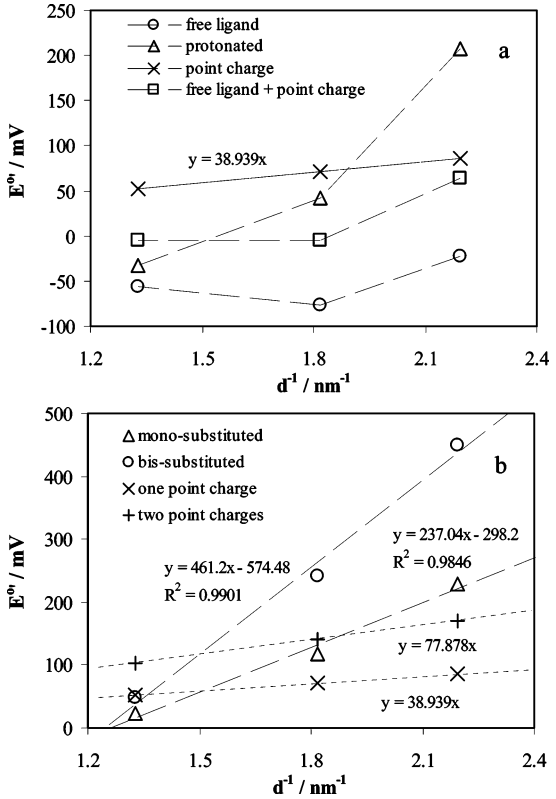

Figure 6. (a) Variation of the mean potential (vs Fc/Fc^+) of the free ligand molecule (○) and its fully protonated form (△) with the reciprocal of the Fe• • •N distance.[7] The calculated mean potentials (×) and their sum with that of the free ligands (□) are also plotted of a simple ferrocene molecule under the influence of a nearby positive point elementary charge. (b) Linear correlations between the mean potential shift and the reciprocal of the Fe• • •N distance for the monosubstituted (△) and bis-substituted (○) ligand molecules, in comparison with the calculated potential shifts due to one (×) and two (+) positive point elementary charges.

lines at the *x* axis, see Figure 6b, eqs 1 and 2 have been derived, according to which the relative permittivity of the local medium around the molecule varies with the length of the alkyl spacer.[4]

$$\Delta E^\circ = \left(\frac{n\Delta Q_{Fc}}{4\pi\epsilon_0 e}\right)\left(\frac{Q_{cation}}{\epsilon d}\right) = A\left(1 - \frac{d}{d_{max}}\right)\frac{Q_{cation}}{l} \qquad (1)$$

$$\frac{1}{\epsilon} = \frac{4\pi\epsilon_0 e}{n\Delta Q_{Fc}} A\left(1 - \frac{d}{d_{max}}\right) \qquad (2)$$

where n is the number of bound cations of equidistance from the ferrocene center, ΔQ_{Fc} is the variation in effective charge on the ferrocene moiety upon the transfer of one electron, d is the distance between the bound cation and the ferrocene center, ϵ_0 is the vacuum permittivity, ϵ is the relative permittivity of the local medium between the bound cation and the ferrocene center, e is the elementary charge, Q_{cation} is the effective charge on the bound cation, and A and d_{max} are both parameters determined by the environment and framework of the molecule. Particularly, the physical meaning of d_{max} is the maximum interaction distance between the ferrocene center and the bound cation at which the potential shift ($\Delta E^{\circ\prime}$) drops to zero. In other words, beyond this length, the intramolecular electrostatic interactions are ineffective.

For the ligands studied here, the value of d_{max} was found to be around 1 nm.[4] This unique finding was not fully understood, although it was thought to be related to the framework and

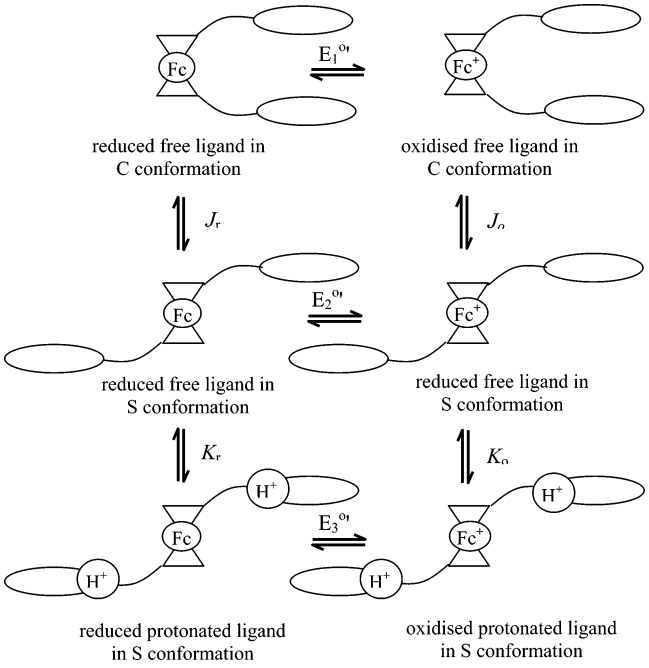

Figure 7. Schemes of two squares showing the relation between mean potentials ($E^{\circ\prime}$) and possible protonation induced conformational changes of the bis-substituted molecules. Other conformations between *C* and *S* may also coexist. *J* and *K* are equilibrium constants of the respective processes.

environment of the ligand molecule.[4] Linking with the above discussion on Figure 6a, it then becomes clear that the term $A(1 - d/d_{max})$ in eqs 1 and 2 actually reflects the proposed through-bond electrostatic interaction. In other words, the alkyl spacer with the tertiary amine may be considered as at least one important part of a "polarizable" local dielectric medium through which electrostatic communication is feasible but also adjustable.

Protonation and Conformational Changes. In solution, substituents on ferrocene can rotate around the Cp−Fe−Cp axis (Cp, the cyclopentadienyl ring) to give various more favorable conformation isomers.[18a] Also, flexible substituents, such as alkyl chains and crown ethers, may undergo folding and stretching.[18c] Therefore, in the presence of different intra- and/or intermolecular forces, for example, electrostatic and/or steric repulsions, the molecules may adopt different conformations and hence exhibit different electrochemical properties. For example, in an early report, the mean potential variation was described when a bipyridinium bis(benzo-crown-ether) ligand formed a 1:1 sandwich complex with large cations and a 1:2 stretched complex with small cations.[24] Similar coordination behavior is expected for **6**a−**6**c. In Figure 7 is illustrated, by the scheme of squares, the influence of cation binding (protonation) induced conformational change on $E^{\circ\prime}$. The *S* and *C* conformations in Figure 7 were observed previously in similar ferrocene bis-crown-ether molecules upon cation complexation.[7c−e] NMR studies in this work also showed similar results: the bis-substituted molecules formed the 1:1 sandwich complex (*C* conformation) and the 1:2 stretched conformation (*S* conformation) with the K^+ ion (see the Supporting Information). The question is whether these conformations apply to the free ligand molecules. Answers to this question are important for the interpretation of the potential data because while the electrostatic interaction determines the difference between E_3° and E_2°, cyclic voltammetry measures that between E_3° and E_1°. It is worth pointing out that a similar scheme can be drawn, starting with the free ligand in the *S* conformation and ending with the

complex in the *C* conformation (i.e., the 1:1 cation−ligand sandwich complex[7d,e]). However, for the free ligand molecules, little conformational information is available in the literature, and both *C* and *S* conformations are only hypothetic limits of the conformational changes between which others may be preferred or could coexist at equilibrium.

Ideally, the use of rigid analogous molecules to **3**a−**3**c and **6**a−6c can make it more straightforward for the study of the above-mentioned conformational changes. While it is still challenging, if not impossible, to synthesize such rigid molecules with alkyl chains, crown ethers, and ferrocene, the fully protonated forms of **3**a−**3**c and **6**a−6c may be considered as satisfactory approximates. First, the flexibility of the crown-ether ring is reduced by the rigid 1,2-oxy-benzene moiety.[4] In addition, for **6**a.$2H^+$−**6**c.$2H^+$, the electric repulsion between the two protons bound to the tertiary amines would not only prevent the substituents from free rotation around the Cp−Fe−Cp axis but also force the alkyl chain into a more stretched conformation. In other words, **6**a.$2H^+$−**6**c.$2H^+$ are in the *S* conformation, as shown in Figure 7. Even for **3**a−**3**c, repulsion between the oxidized ferrocene center and the bound proton may also cause stretching.

The conformational conversions mentioned above change the shape and size (length) and hence the diffusion behavior of the molecule according to the work of Stokes and Einstein[25a] and others.[25b] In summary, the diffusion coefficient (*D*) is related to the molecular geometry by the following equation

$$D = kT/f \tag{3}$$

where *k* is the Boltzmann constant, *T* is the temperature, and *f* is the frictional coefficient which is a function of the molecular geometry and solution viscosity. For a solvated spherical molecule of radius *r* in a solution of viscosity η, $f = 6\pi\eta r$ and eq 3 becomes the Stokes−Einstein equation.[25a]

$$D = kT/6\pi\eta r \tag{4}$$

Note that eq 4 applies to both charged and neutral diffusing molecules.[25a] For nonspherical molecules, *f* varies from that in eq 4. In this work, the acetonitrile solutions remained very similar to each other, and so did the viscosity. The solvated molecules can be approximated as ellipsoids in shape. It has been found that when the ratio of the long and short axes of the ellipsoid changes from 1 to 4, *f* increases slightly to less than 20% of that of a sphere of the same volume.[25b] Therefore, the Stokes−Einstein equation can still be applied with satisfactory accuracy to evaluate the sizes of our molecules (and other similar supramolecules) from the diffusion coefficients that can be measured by cyclic voltammetry.

As illustrated in Figure 7, the *S* conformation is longer and hence diffuses slower than the *C* conformation (or others between the two) in solution. Obviously, the conversion between the *S* and *C* conformations is only applicable to the bis-substituted ferrocene molecules (**6**a−**6**c). However, because the monosubstituted ones (**3**a−**3**c) have effectively the same length as the *C* conformation, their diffusion behavior can be used as the reference for judging the occurrence of the *C* or other possible conformations in **6**a−**6**c.

For a reversible electron transfer process at 25 °C, the voltammetric peak current of the forward potential sweep on a planar electrode is linked to the diffusion coefficient of the redox species by the following equation[25c,d]

$$i_p = 2.69 \times 10^5 n^{3/2} D^{1/2} \upsilon^{1/2} c^* \tag{5}$$

where i_p is the peak current density (A cm^{-2}), *n* is the number of transferred electrons, υ is the potential scan rate (V s^{-1}), and c^* is the concentration (mol cm^{-3}) of the redox species in the electrolyte. The diffusion coefficient (*D*) is in the units of cm^2 s^{-1}. Equation 5 predicts linear relationships of the peak current against the square root of the scan rate at a given concentration, or against the ligand concentration at a given scan rate. The slopes of these straight lines can then be used to calculate the diffusion coefficients.

Considering possible influences of experimental errors such as weighing the semisolid or oily samples (see the Experimental Section) at the milligram scale and adsorption on electrodes (see Figure 2 and the relevant discussion), a large number of *D* values were derived from the voltammetric currents, and the averages are given in Table 1. Some points are worth mentioning. First, the *D* values of the monosubstituted molecules are approximately twice as large as those of the bis-substituted ones. It indicates (1) similar conformations for the substituents in the bis- and monosubstituted molecules and, more importantly, (2) the bis-substituted ligands being in the *S* conformation, in agreement with the steric repulsion. Second, the results do not show a clear difference in *D* values between the free and protonated ligands, implying little effect from the electric repulsion between the two bound protons to further stretch the molecule. In other words, the unprotonated bis-substituted molecules were already in the *S* conformation and stretched, which could only result from the steric repulsion. Finally, increasing the alkyl chain length resulted in only fractional changes in the *D* values of the free ligands, and the differences were unfortunately within the experimental error encountered in this work.

The above analysis and discussion on diffusion coefficients impress an insignificant difference between the conformations of the free and protonated ligand molecules in acetonitrile. Consequently, for these molecules, either there is no difference between $E_1^{\circ\prime}$ and $E_2^{\circ\prime}$ in Figure 7 or the *S* conformation is more favored on the time scale of voltammetry due to the steric repulsion. This understanding agrees with the observed linear correlations between $\Delta E^{\circ\prime}$ and the reciprocal of the distance between the centers of the bound cation and the ferrocene group, as those shown in Figure 6b, or the bound cation's effective charge.[4,8d] In agreement with this electrochemical finding, ^{1}H NMR studies in CD_3CN and $CDCl_3$ also revealed that the bis-substituted molecules were in the *S* conformation (see the Supporting Information).

Finally, it is evident from the literature that structures and conformations of supramolecules are often determined by solid-state techniques, such as X-ray crystal analysis, but the results may be arguable for the same molecules in solution.[7a,b] Advanced NMR methods (e.g., 2D NOESY NMR) are a suitable alternative and will be pursued in our ongoing research. On the other hand, electrochemical means are quicker, cheaper, and easier to use and capable of providing qualitative and/or semiquantitative conformational information of supramolecules in solution to complement that from more sophisticated techniques.

Conclusion

With systematic variation of the alkyl spacer length in ferrocene benzoaza-15-crown-5 receptor molecules, voltammetric measurements of the molecules before and after protonation revealed an enhanced mean potential variation. This enhancement implies that the alkyl spacer, particularly a short one, may be capable of providing a pathway for through-bond

electrostatic interaction between the ferrocene and the protonated tertiary amine. This implication differs from the conventional concept that an alkyl chain is an insulator for electrostatic communication. In terms of Coulomb's law, the through-bond interaction can be incorporated into the relative permittivity, which compares the alkyl chain as one important part of a polarizable local dielectric medium through which electrostatic communication can proceed. Further, the diffusion coefficients of the molecules varied only fractionally before and after protonation, as determined by cyclic voltammetry, indicating that electric repulsion has a very limited effect, if any, to further stretch the molecules in addition to what has already been done by steric repulsion. This is evidence of these molecules adopting reasonable stable conformations in solution, although they consist of flexible substituents (alkyl chains + crown-ether rings) that could, under influence, rotate around the Cp−Fe−Cp axis of the ferrocene moiety.

Acknowledgment. We thank the Natural Science Foundation of China (Grant No. 20125308) for financial support and the Ministry of Education of China for a Cheung Kong Scholarship to G.Z.C.

Supporting Information Available: Tables and figures showing MALDI-TOF-MS and NMR characterizations of the molecules and discussion on a ^{1}H NMR investigation on conformational changes in solution. This material is available free of charge via the Internet at http://pubs.acs.org.

References and Notes

(1) Beer, P. D. *Chem. Soc. Rev.* **1989**, *18*, 409. (b) Boulas, P. L.; Gomez-Kaifer, M.; Echegoyen, L. *Angew. Chem., Int. Ed. Engl*. **1998**, *37*, 216. (c) Beer, P. D.; Gale, P. A.; Chen, G. Z. *Adv. Phys. Org. Chem*. **1998**, *31*, 1.

(2) Hall, C. D.; Kirkovits, G. J.; Hall, A. C. *Chem. Commun.* **1999**, 1897.

(3) (a) Beer, P. D.; Gale, P. A.; Chen, Z.; Drew, M. G. B.; Health, J. A.; Ogden, M. I.; Powell, H. R. *Inorg. Chem*. **1997**, *36*, 5880. (b) Ion, A. C.; Moutet, J.-C, Pailleret, A.; Popescua, A.; Saint-Aman, E.; Siebert, E.; Ungureanua, E. M. *J. Electroanal. Chem*. **1999**, *464*, 24. (c) Ion, I.; Moutet, J. C.; Popescu, A.; Saint-Aman, E.; Tomazeswski, L.; Gautier-Luneau, I. *J. Electroanal. Chem.* **1997**, *440*, 1997. (d) Ion, A.; Ion, I.; Popescu, A.; Ungureanu, M.; Moutet, J. C.; SaintAman, E. *Adv. Mater*. **1997**, *9*, 711. (e) Beer, P. D.; Crowe, D. B.; Ogden, M. I.; Drew, M. G. B.; Main, B. *J. Chem. Soc., Dalton. Trans.* **1993**, 2107.

(4) Jin, S.; Wang, D. H.; Jin, X. B.; Chen, G. Z. *ChemPhysChem* **2004**, *5*, 1623.

(5) (a) Beer, P. D.; Gale, P. A.; Chen, G. Z. *J. Chem. Soc., Dalton. Trans*. **1999**, 1897. (b) Beer, P. D.; Gale, P. A. *Angew. Chem., Int. Ed. Engl.* **2001**, *40*, 487. (c) Gale, P. A. *Coord. Chem. Rev.* **2003**, *240*, 191.

(6) (a) Hall, C. D.; Sharpe, N. W.; Danks, I. P.; Sang, Y. P. *J. Chem. Soc., Chem. Commun.* **1989**, 419. (b) Medina, J. C.; Goodnow, T. T.; Rogers, M. T.; Atwood, J. L.; Lynn, B. C.; Kaifer, A. E.; Gokel, G. W. *J. Am. Chem. Soc*. **1992**, *114*, 10583. (c) Chen, Z.; Gale, P. A.; Health, J. A. and Beer, P. D. *J. Chem. Soc., Faraday Trans*. **1994**, *90*, 2931.

(7) (a) Plenio, H.; Yang, J.; Diodone, R.; Heinze, J. *Inorg. Chem.* **1994**, *33*, 4098. (b) Plenio, H.; Diodone, R. *Inorg. Chem*. **1995**, *34*, 3964. (c) Beer, P. D.; Chen Z.; Drew M. G. B.; Pilgrim, A. *Inorg. Chim. Acta* **1994**, *225*, 137. (d) Beer, P. D.; Sikanyika, H.; Slawin, A. M. Z.; Williams, D. J. *Polyhedron* **1989**, *8*, 879. (e) Beer, P. D.; Danks, J. P.; Hesek, D.; McAleer, J. F. *J. Chem. Soc., Chem. Commun.* **1993**, 1735.

(8) (a) Hall, C. D.; Chu, S. Y. F. *J. Organomet. Chem.* **1995**, *498*, 221. (b) Benito, A.; Martínez-Máñez, R.; Soto, J.; Tendero, M. J. L. *J. Chem. Soc., Faraday Trans.* **1997**, *93*, 2175. (c) Chen, Z.; Pilgrim, A. J.; Beer, P. D. *J. Electroanal. Chem*. **1998**, *444*, 209. (d) Plenio, H.; Aberle, C.; Shihadeh, Y. A.; Lloris, J. M.; Martínez-Máñez, R.; Pardo, T.; Soto, J. *Chem.−Eur. J.* **2001**, *7*, 2848.

(9) Kumar, S.; Nussionv, R. *ChemBioChem* **2002**, *3*, 604.

(10) Kuby, J. *Immunology*; W. H. Freeman and Company, New York, 1992; p 121.

(11) (a) Bdjic, J. D.; Balzani, V.; Credi, A.; Silvi, S.; Stoddart, J. F. *Science* **2004**, 303, 1845. (b) Hawthorne, M. F.; Zink, J. I.; Skelton, J. M.; Bayer, M. J.; Liu, C.; Livshits, E.; Baer, R.; Neuhauser, D. *Science* **2004**, *303*, 1849.

(12) (a) Benkeser, R. A.; Goggin, D.; Schroll, G. *J. Am. Chem. Soc.* **1954**, *76*, 4025. (b) Rausch, M. D.; Ciappenelli, D. J. *J. Organomet. Chem.* **1967**, *10*, 127. (c) Graham, P. J.; Lindsey, R. V.; Parshall, G. W.; Peterson, M. L.; Whitman, G. M. *J. Am. Chem. Soc*. **1957**, *79*, 3416. (d) Rinehart, K. L., Jr.; Curby, R. J., Jr.; Sokol, P. E. *J. Am. Chem. Soc*. **1957**, *79*, 3420. (e) Nesmeyanov, A. N.; Vol'kenau, N. A.; Vil'chevskaya, V. D. *Dokl. Akad. Nauk. SSSR* **1956**, *111*, 362.

(13) Grossel, M. C.; Hamilton, D. G.; Fuller, J. I.; Millan-Barios, E. *J. Chem. Soc., Dalton Trans.* **1997**, 3471.

(14) Dong, T. Y.; Chang, C. K.; Cheng, C. H.; Lin, K. J. *Organometallics* **1999**, *18*, 1911.

(15) Lu, T. B.; Wu, C. T. *Org. Chem*. **1985**, *4*, 312.

(16) Ledricer, D.; Hauser, C. R. *Org. Synth*. **1960**, *40*, 31.

(17) Beer, P. D.; Chen, Z.; Drew, M. G. B.; Kingston, J.; Ogden, M. I.; Spencer, P. *J. Chem. Soc., Chem. Commun*. **1993**, 1046.

(18) (a) Long, N. J. *Metallocenes: An Introduction to Sandwich Complexes*; Blackwell Science: Oxford, U.K., 1998; p 134. (b) Dietz, S. D.; Bell, W. L.; Cook, R. L. *J. Organomet. Chem.* **1997**, *545−546*, 67. (c) Morrison, R. T.; Boyd, R. N. *Organic Chemistry*, 5th ed.; Allyn and Bacon, Inc.: London, 1987; pp 83, 147, and 710.

(19) (a) Beer, P. D.; Chen, Z.; Ogden, M. I. *J. Chem. Soc., Faraday Trans*. **1995**, *91*, 295. (b) Chen, Z.; Graydon, A. R.; Beer, P. D. *J. Chem. Soc., Faraday Trans.* **1996**, *92*, 97. (c) Reynes, O.; Moutet, J.-C, Royal, G.; Saint-Aman, E. *Electrochim. Acta*, **2004**, *49*, 3727. (d) Reynes, O.; Maillard, F.; Moutet, J. C.; Royal, G.; Saint-Aman, E.; Stanciu, G.; Dutasta, J. P.; Gosse, I.; Mulatier, J. C. *J. Organomet. Chem.* **2001**, *637*, 356.

(20) Hultgren, V. M.; Mariotti, A. W. A.; Bond, A. M.; Wedd, A. G. *Anal. Chem*. **2002**, *74*, 3151.

(21) (a) Kondo, T.; Takechi, M.; Sato, Y.; Uosaki, K. *J. Electroanal. Chem*. **1995**, *381*, 203. (b) Stone, D. L.; Smith, D. K. *Polyhedron* **2003**, *22*, 763.

(22) Coutouli-Argyropoulou, E.; Kelaidopoulou, A.; Sideris, C.; Kokkinidis, G. *J. Electroanal. Chem*. **1999**, *477*, 130.

(23) (a) Corbridge, D. E. C., *Phosphorus*—An Outline of its Chemistry, Biochemistry and Technology, 3rd ed.; Elsevier: Oxford, U.K., 1985; p 107. (b) Larson, J. W.; Su, B. L. *J. Chem. Eng. Data* **1994**, *39*, 33. (c) Larson, J. W., Su, B. L. *J. Chem. Eng. Data* **1994**, *39*, 36.

(24) Beer, P. D.; Chen, Z.; Grave, A.; Haggitt, J. *J. Chem. Soc., Chem. Commun*. **1994**, 2413.

(25) (a) Atkins, P. W. *Physical Chemistry*, 2nd ed.; Oxford University Press: Oxford, 1982; p 905. (b) Tinoco, I.; Sauer, K.; Wang, J. C. *Physical Chemistry. Principles and Applications to the Biological Sciences*; Prentice Hall: Upper Saddle River, NJ, 1978; pp 212−219. (c) Bard, A. J.; Faulkner, L. R. *Electrochemical Method−Fundamentals and Applications*, 2nd ed.; John Wiley & Sons Inc.: New York, 2001; p 231. (d) Asakawa, T.; Sunagawa, H.; Miyagishi, S. *Langmuir* **1998**, *14*, 7091.

(26) Gokel, G. W. In *Crown Ethers & Cryptants*; Stoddart, J. F., Ed.; The Royal Society of Chemistry: Cambridge, U.K., 1994.